www.cadanda.com
Computer-Aided Design AND APPLICATIONS

Optimization of Barrel Cutter for Five-axis Flank-milling Based on Approximation of Tool Envelope Surface

Dongqing Yan[1], Dinghua Zhang[2] and Ming Luo[3]

[1]Northwestern Polytechnical University, dawnyan@mail.nwpu.edu.cn
[2]Northwestern Polytechnical University, dhzhang@nwpu.edu.cn
[3]Northwestern Polytechnical University, luoming@nwpu.edu.cn

ABSTRACT

This paper fit the parameter model of barrel cutter approaching to the design surface with the spatial point cloud by approximation theory. There are two principle parameters determining the envelope surface shape of barrel cutter: the radius of the generatrix curve and the maximum rotating radius, therefore the main work in this paper is optimizing the two parameters for strip-width-maximization machining, aiming at maximizing processing bandwidth with the sum of the unsigned deviations between the cutter envelop surface and the designed surface within the allowance. Detailed analysis of the relevance between the two parameters and machining error is introduced. Then, the optimum parameters of cutter are determined through the application of the least squares method (LS). Computer implementations are presented to verify the effectiveness and accuracy of the proposed method.

Keywords: barrel cutter, envelope surface, flank milling, strip-width-maximization machining.

1. INTRODUCTION

Flank milling involves machining a workpiece with the side part of the cutter. The cutter generatrices are generally straight lines (cylindrical cutter or conical cutter) or arcs of circles (barrel cutter). Compared with point milling, flank milling has its unique advantages. It can increase the material removal rate, eliminate necessary hand finish and ensure improved component accuracy. Thus increasing attention was drawn onto the problem of optimum positioning of the cutter for flank milling. It's well known that the machined surface in flank milling is formed by the swept envelope of the cutter surface. The actual machining errors are the deviations between the cutter envelope surface and designed surface. The primary problem of increasing the machining precision is to approach the tool envelope surface to designed surface as close as possible. However, lots of papers focus on the optimization of tool paths from the perspective of increasing machining accuracy, avoiding interference or reducing cutting force with fixed cutter. Only a few works address the problem of increasing machining precision by approximating the cutter envelope surface to designed surface.

Wang et al. [16] proposed a flank milling tool positioning method based on an offset point of the designed surface with the excess error is nearly equal to the allowed error. The slip angle and yaw angle were adjusted to find the optimized tool position. Chaves-Jacob et al. [6] proposed a novel approach (Computation of Adapted Tool Shape) that optimizes the tool shape for a given trajectory-surface pair to reduce the interferences. Chu et al. [9] use a developable surface to approximate an undevelopable ruled surface for avoiding interference. The theoretical machining error is just the approximation error. Yang et al. [19] proposed a method to approximate swept volumes of NURBS surfaces or solids by slicing NURBS surfaces into sliced curves and finding the characteristic point in a moving frame. Maeng et al. [14] presented a Z-map update method to calculate the envelope surface for linearly moving tools. This method can calculate the undercut and overcut for machining simulation directly. Chung et al. [10] proposed a method using a single valued function to represent the cutter swept surface (CSS) for a generalized cutter, which can only be used in 3-axis machining. Gong et al. [12,13] determined the optimum CL by

Taylor & Francis
Taylor & Francis Group

least squares (LS) fitting of a spatial line to a series of post-processed point data. This method could smooth the error distribution in the normal section along the feed direction, but it can't control the errors between the cutter envelope surface and design surface in regions near the contact point. Chiou [7,8] presented a closed-form solution of the swept profile of the APT cutters for the simulation of 5-axis machining. Weinert et al. [18] proposed an analytical method to calculate the swept profile of a fillet-end cutter for five-axis NC-milling based on the moving frame method. Du et al. [11] extended this method to generalized (APT) cutters with several different formulas for different cutters, such as fillet-end, ball-end and flat-end.

Blackmore et al. [2,3] proposed a swept envelope differential equation (SEDE) to characterize swept volume boundaries and reduce the computation complexity. Wang et al. [17] used the tangency condition and moving frame method to calculate a family of critical curves for modeling the swept volume. Abdel-Malek et al. [1] proposed an implicit equation to determine the swept profile by using the Jacobian rank-deficiency condition. Park et al. [15] proposed a hybrid cutting simulation based on a discrete vector model and vector intersection. Bohez et al. [4] presented an algorithm based on the sweep plane approach to determine the machined part geometry in 5-axis machining with general APT tools. Rossignac et al. [5] used a poly screw approximation of the motion to compute the swept boundary for a free-form solid.

All the above methods focus on optimizing the tool positions with the tool shape being fixed. From the opposite perspective, a new method to optimize the tool shape for five-axis flank milling is presented in this paper. The machined surface in flank milling is formed by the swept envelope of the cutter surface. The actual machining errors are the deviations between the cutter envelope surface and the designed surface. Transferring the designed surface into spatial point cloud and the optimum tool shape can be obtained by approximation theory with the deviations between the cutter envelope surface and the spatial point cloud within error tolerance. The rest of this paper is organized as follows. In Section 2, the principle of the new optimization method is introduced in detail. Then, several examples and discussions are presented in Section 3. In the end, the conclusions are given in Section 4.

2. NEW OPTIMIZATION METHOD OF BARREL CUTTER FOR FLANK MILLING

Barrel cutter is a rotary cutter which is enclosed by a surface of revolution. As shown in Fig. 1, the cutter surface is generated by rotating a generatrix (arc of circle) on the $\mathbf{y}-\mathbf{z}$ plane around the y-axis. The tool shape is determined by the arc length and radius of the generatrix as well as the maximum rotating radius. However, only the two latter parameters affect the mesh condition between the tool envelope surface S_c and the designed surface S. According to Section 1, we know that the true machining errors ε_i are the distances between the cutter and the designed surface. Thus the main task in this method is optimizing the two principle parameters to make the sum of the unsigned deviations between the cutter envelop surface and the designed surface the smallest.

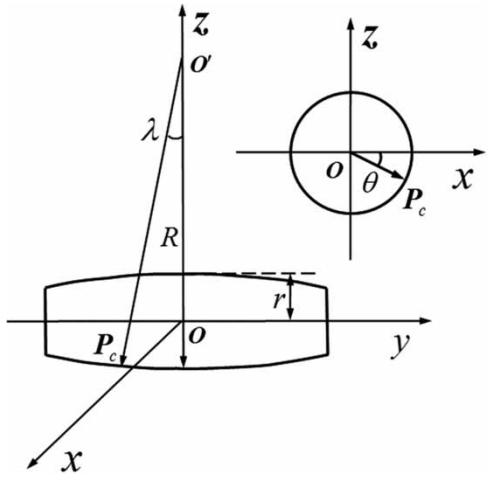

Fig. 1: Geometrical definition of barrel cutter.

2.1. Geometric Model of Barrel Cutter

As shown in Fig. 1, the local tool Cartesian coordinate system is represented by $(\mathbf{x},\mathbf{y},\mathbf{z})$ where O is the tool center and $\mathbf{y}$ is the unit principle direction along the tool axis. In this coordinate system, the coordinates (x_c,y_c,z_c) of the point P_c in tool envelope surface can be expressed as

$$\begin{cases} x_c = r_c \cdot \cos\theta \\ z_c = r_c \cdot \sin\theta \\ r_c = \sqrt{R^2 - y_c^2} - (R - r) \end{cases} \tag{1}$$

where parameter R and r denote the radius of the generatrix and the maximum rotating radius respectively. Parameter r_c denotes the rotating radius of the tool surface at point P_c. The maximum value of r_c is the maximum rotating radius which is one of the principle parameters to be optimized.

The system of equations above can be expressed as an equation without parameter r_c which presents the envelop surface of the cutter $S_c(x_c, y_c, z_c)$:

$$\sqrt{x^2 + z^2} = \sqrt{R^2 - y^2} - (R - r) \tag{2}$$

In Eq.(2), the coordinate (x_c, y_c, z_c) is only associated with parameter R and r. While the values of R and r are determined, the shape of the tool envelope surface S_c is confirmed.

2.2. Relevance between the Tool Envelope Surface and the Machining Error

As we all know, there are two expressions for error. In ISO standard, the definition of error is the distance between the designed surface S and the tool envelope surface S_c along the normal direction of the designed surface, as shown in Fig. 2(a). This definition of error is widely used to evaluate the machining precision in industry. The other definition of error is the distance between the designed surface S and the tool envelope surface S_c along the normal direction of the tool envelope surface, as shown in Fig. 2(b). Obviously, the definition of error is very vital to the final optimized result because it is the key link between the tool envelope surface and the designed surface. In this paper, the deviations between S and S_c are calculated based on the definition of error in the ISO standard.

As a free surface can always be approximated by a point cloud, in the proposed method, the designed surface S is transferred into isoparametric discrete points. Hence the computation of the signed deviation between S and S_c is transferred into that of the distance from point cloud to cuttr surface S_c. According to the differential geometry, the coordinates (x_s, y_s, z_s), unit normal vector $\mathbf{n}(n_0, n_1, n_2)$ and principle radiuses of these discrete points on designed surface can be acquired from the geometric model of S. Based on the adaptive curvature match, the initial tool surface S_0 can be obtained according to the curvature information of the discrete points. Furthermore, these points can be seen as the contact points and they are also the initial points used to fit the tool envelope surface S_c. In consideration of the amount of points, to improve the computational efficiency, we choose the discrete points in the parameter curves every t points as the contact points P_s for optimization where t is the number of the neglected points.

The relative position between the designed surface and cutter surface is exceedingly important while modeling the tool envelope surface at contact point P_s. As shown in Fig. 1, the envelop surface of the barrel cutter is generated in the coordinate system (x_c, y_c, z_c). In this method, an initial position should be given for the calculation of initial ε_i. According to the analysis of differential geometry, as the minimum principal directions of S and S_c are coincident, the strip width gets to the largest. Consequently, the principle position and gesture of the cutter is set as shown in Fig. 3. $\mathbf{e}_1$ and $\mathbf{e}_2$ denote the the maximum and minimum principle directions of the designed surface at contact point P_c respectively. The vectors of $\mathbf{n}(n_0, n_1, n_2)$, $\mathbf{e}_1$ and $\mathbf{e}_2$ are orthogonal to each other. Meanwhile, the directions of the maximum and minimum principle curvature of the barrel cutter are parallel. So the direction of $z-axis$ is adjusted along the unit normal vector $\mathbf{n}(n_0, n_1, n_2)$ through the contact point and direction of $x-axis$ and $y-axis$ is set along the vectors of the principle curvatures $\mathbf{e}_1$, $\mathbf{e}_2$ respectively.

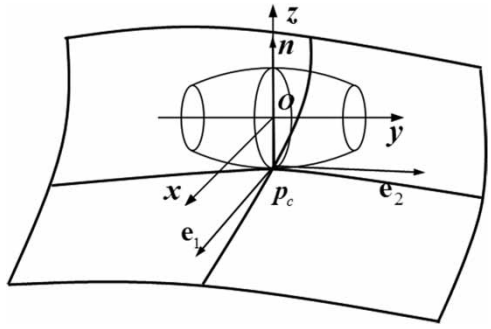

Fig. 3: Relative position between the designed surface and cutter surface.

After the determination of initial the relative position, then, the deviations ε_i between the tool envelop surface S_c and the discrete points near P_s can be calculated by the association among (x_c, y_c, z_c), (x_s, y_s, z_s), $\mathbf{n}(n_0, n_1, n_2)$ and ε_i. According to the definition of ε, the association can be described as

$$P_c - P_s = \varepsilon_i \mathbf{n} \tag{3}$$

$$(x_c - x_s, y_c - y_s, z_c - z_s) = \varepsilon_i (n_0, n_1, n_2) \tag{4}$$

From the transformation of Eq. (3), we can achieve an equation system expressing the coordinates (x_c, y_c, z_c)

$$\begin{cases} x_c = x_s + \varepsilon_i n_0 \\ y_c = y_s + \varepsilon_i n_1 \\ z_c = z_s + \varepsilon_i n_2 \end{cases} \tag{5}$$

substituting Eq. (4) into Eq. (2),

$$\sqrt{(x_s + \varepsilon_i n_0)^2 + (z_s + \varepsilon_i n_2)^2} = \sqrt{R^2 - (y_s + \varepsilon_i n_1)^2} - (R_0 - r_0) \tag{6}$$

where parameter R_0 and r_0 of initial tool surface S_0 are known quantities. So in Eq. (5), ε_i is the only

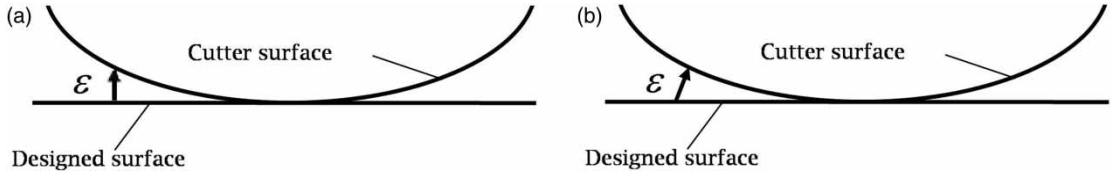

Fig. 2: The definitions of machining error.

unknown quantity and the other parameters are all known. Seen from the form of the equation, Eq. (5) can be transferred into a quartic equation with one unknown:

$$
\begin{aligned}
&a\varepsilon_i^4 + b\varepsilon_i^3 + c\varepsilon_i^2 + d\varepsilon_i + e = 0\\
&\quad a = (n_0^2 + n_1^2 + n_2^2)^2\\
&\quad b = 4(n_0^2 + n_1^2 + n_2^2)(x_s n_0 + y_s n_1 + z_s n_2)\\
&\quad c = 2[2(x_s n_0 + y_s n_1 + z_s n_2)^2\\
&\qquad + (x_s^2 + y_s^2 + z_s^2)(n_0^2 + n_1^2 + n_2^2)\\
&\qquad - (r^2 + 2R^2 - 2Rr)(n_0^2 + n_2^2) + (r^2 - 2Rr)n_1^2]\\
&\quad d = 4[(x_s^2 + y_s^2 + z_s^2)(x_s n_0 + y_s n_1 + z_s n_2) - (r^2 + 2R^2\\
&\qquad - 2Rr)(x_s n_0 + z_s n_2) + (r^2 - 2Rr)y_s n_1]\\
&\quad e = (x_s^2 + y_s^2 + z_s^2)^2 - 2(r^2 + 2R^2 - 2Rr)(x_s^2 + z_s^2)\\
&\qquad + 2(r^2 - 2Rr)y_s^2 + (r^2 - 2Rr)^2
\end{aligned}
\tag{7}
$$

The ε_i can be calculated by solving the equation above in virtue of the root formula of quartic equation with one unknown.

Not all the discrete points are suitable for approximation. To choose the convenient points, a limit δ is confirmed while all the ε_i are achieved, the points $P_i(\varepsilon_i \le \delta, 0 \le i \le n)$ are reserved as the initial data points for fitting. There is one significant point requiring attention that if the ε_i is negative and out of limit, the process of screening is over, of which the purpose is to avoid the happening of overcutting.

2.3. Optimization of Barrel cutter

The primary hope of the new optimization method is that the machined surface approximates to the designed surface as close as possible. In this paper, we adopt least squares (LS) criterion to solve the approximation problem, which can be expressed as

$$\min E = \frac{1}{n}\sum_{i=1}^{n}\varepsilon_i^2 \tag{8}$$

ε_i denotes the machining error at point P_s.

Obviously, iteration is needed to obtain the optimum parameters. The surface S' of new tool envelope surface after the first fitting process can be seen as the new initial envelope surface S_0 for next optimization, and repeat the process above until

$$|E_{i+1} - E_i| \le \xi \tag{9}$$

which means the calculated result become stable with the growth in the number of iterative calculations. ξ denotes the iteration tolerance.

The optimization of tool parameters at one contact point is implemented as described above and a local optimized barrel cutter can be achieved. However, for the whole design surface S, the optimum parameters R and r are respectively the $R_{\min}$ and $r_{\min}$ among all the computing results at each point P_s aiming at avoiding overcutting. Hence, the iterative computation should be taken all over the designed surface and the minimax of the calculated values are selected as the optimum parameters. The detailed process of this optimization method is shown in Fig. 4.

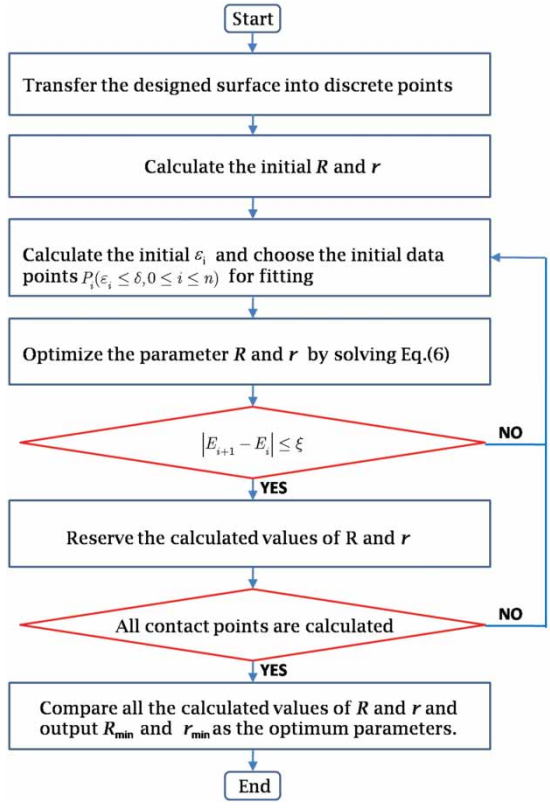

Fig. 4: Flow chart of optimization process for barrel cutter.

3. EXAMPLES AND DISCUSSIONS

In order to demonstrate the validity of the proposed method, we give a simulation of optimization of the barrel cutter for five-axis flank milling of the free-form blade surface shown in Fig. 5.

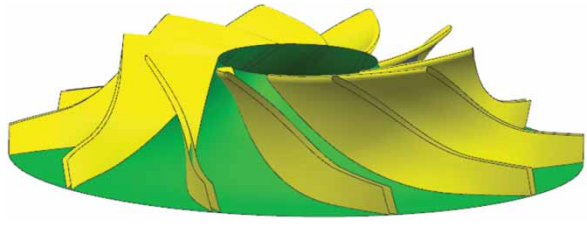

Fig. 5: Blade surface of impeller to be machined with barrel cutter.

According to the analysis above, R and r are the parameters that determine the tool shape. The model of the barrel cutter with ball end is shown in Fig. 6. In this example, the initial values of R and $r$are chosen as 20 mm and 4 mm respectively.

Fig. 6: The model of barrel cutter.

Figure 7 shows the process of the iterative calculation of R and r at the point $P_{0.35,0.4}$ (u = 0.35, v = 0.4) and $P_{0.4,0.2}$ (u = 0.4, v = 0.2).

For point $P_{0.35,0.4}$, the value of R are 20.000, 50.765, 50.299, 50.269 and the value of r are 4, 5, 6, 7. For point $P_{0.4,0.2}$, the value of R are 20.000, 91.580, 51.788, 51.449, 51.512 and the value of r are 4, 24.646, 25.646, 26.646, 27.646. Seen from Fig. 7, R and r approach stable after only three or four iterations, which shows the iteration speed of the method in this paper is fast and effective.

Calculate all the discrete points on the designed surface and round the calculated values of $R_{\min}$ and $r_{\min}$. The optimum parameters of barrel cutter for blade surface in Fig. 5 are achieved as $R = 50$ and r=5. For impeller, the distance d between the adjacent blades of the impeller should be taken into account when choose the parameter r of the cutter. r must be smaller than d. The smallest distance of the adjacent blades in this example is 11.735 mm which is larger than the calculated value of r.

Simulating processing for blade surface with the optimized tool is implemented to validate the optimization method. Fig. 8 shows the tool paths of with the initial cutter and the optimized cutter.

The total length of the tool path with the initial cutter is 874.5389 mm and the length with optimized barrel cutter is 656.7897 mm. Comparing the length of the paths shown in Fig. 7-(b) and Fig 7-(c), the total tool path length with optimized cutter is 24.90% shorter than the tool path before Optimization. The results of the validation show that the proposed optimization method of barrel cutter can greatly improve the machining efficiency, reduce the polish work and increase the surface integrity.

4. CONCLUSIONS

This paper proposed a tool parameter optimization method for five-axis flank milling barrel cutter. Concluding from the validations, we can see that this method can expand the machining bandwidth greatly while controlling the errors between the cutter envelope surface and the designed surface in regions near the contact point. In this method, the tool envelope surface is optimized to approach the design surface by fitting the discrete points near contact point. While the amount of data points is large, the computation is

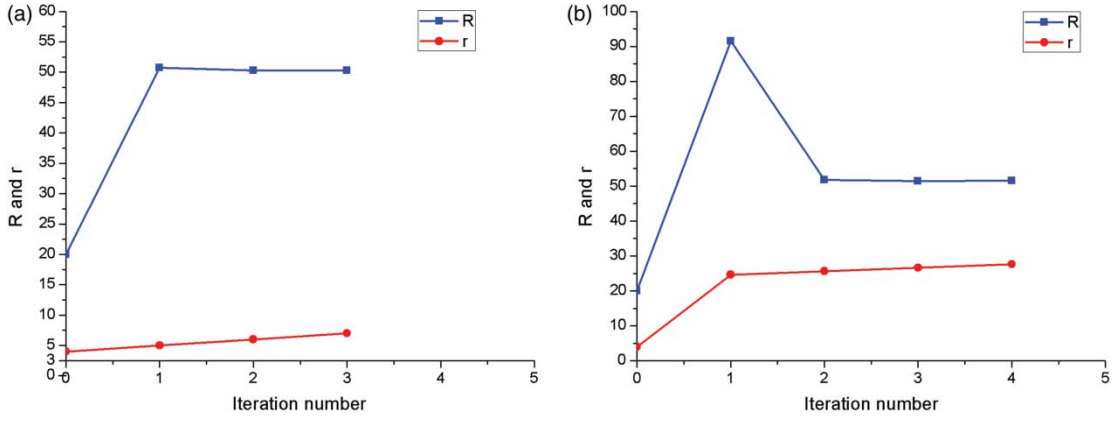

Fig. 7: Optimizations of parameter R and r at point (0.35, 0.4) and point (0.4, 0.2).

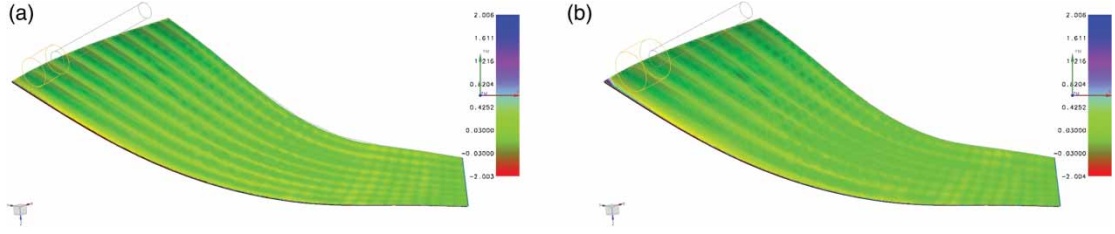

Fig. 8: Simulating processing for blade surface. (a) Tool path with the initial cutter. (b) Tool path with the optimized cutter.

complex in this method, so there exists further study on improving the calculative efficiency.

ACKNOWLEDGEMENTS

The authors would like to thank the anonymous reviewers and all the seniors for their good guidance and helpful suggestions. This work was sponsored by Basic Research Foundation of Northwestern Polytechnical University (Grant No. JCY20130121) and the 111 Project (Grant No. B13044).

REFERENCES

[1] Abdel-Malek, K.; Yeh, H.-J.: Geometric representation of the swept volume using Jacobian rank-deficiency conditions, Computer Aided Design, 29(6), 1997, 457–468. http://dx.doi.org/10.1016/S0010-4485(96)00097-8

[2] Blackmore, D.; Leu, M. C.; Wang, L. P.: The sweep-envelope differential equation algorithm and its application to NC machining verification, Computer Aided Design, 29(9), 1997, 629–638. http://dx.doi.org/10.1016/S0010-4485(96)00101-7

[3] Blackmore, D.; Leu, M. C.; Shih, F.: Analysis and modeling of deformed swept volumes, Computer Aided Design, 26(4), 1994, 315–326. http://dx.doi.org/10.1016/0010-4485(94)90077-9

[4] Bohez, E. L. J.; Minh, N. T. H.; Kiatstrithanakorn, B. et al: The stencil buffer sweep plane algorithm for 5-axis CNC tool path verification, Computer Aided Design, 35(12), 2003, 1129–1142. http://dx.doi.org/10.1016/S0010-4485(02)00209-9

[5] Rossignac, J.; Kim, J. J.; Song, S. C. et al: Boundary of the volume swept by a free-form solid in screw motion, Computer Aided Design, 39(9), 2007, 745–755. http://dx.doi.org/10.1016/j.cad.2007.02.016

[6] Chaves-Jacob, J.; Poulachon, G.; Duc, E.: New approach to 5-axis flank milling of free-form surfaces: computation of adapted tool shape, Computer-Aided Design, 41(12), 2009, 918–929. http://dx.doi.org/10.1016/j.cad.2009.06.009

[7] Chiou, C.-J.; Lee, Y.-S.: Swept surface determination for five-axis numerical control machining, International Journal of Machine Tools & Manufacture, 42(14), 2002, 1497–1507. http://dx.doi.org/10.1016/S0890-6955(02)00110-4

[8] Chiou, C.-J.; Lee, Y.-S.: A shape-generating approach for multi-axis machining G-buffer models, Computer Aided Design, 31(12), 1999, 761–776. http://dx.doi.org/10.1016/S0010-4485(99)00069-X

[9] Chu, C.-H.; Chen, J.-T.: Tool path planning for five-axis flank milling with developable surface approximation, Journal of Advanced Manufacturing Technology, 29(7–8), 2006, 707–713. http://dx.doi.org/10.1007/s00170-005-2564-6

[10] Chung, Y. C.; Park, J. W.; Shin, H. et al: Modeling the surface swept by a generalized cutter for NC-verification, Computer Aided Design, 30(8), 1998, 587–594. http://dx.doi.org/10.1016/S0010-4485(97)00033-X

[11] Du, S. J.; Surmann, T.; Webber, O. et al: Formulating swept profiles for five axis tool motions, International Journal of Machine Tools & Manufacture, 45(7–8), 2005, 849–861. http://dx.doi.org/10.1016/j.ijmachtools.2004.11.006

[12] Gong, H.; Wang, N.: Analytical calculation of the envelope surface for generic milling tools directly from CL-data based on the moving frame method, Computer-Aided Design, 41(11), 2009, 848–855. http://dx.doi.org/10.1016/j.cad.2009.05.004

[13] Gong, H.; Wang, N.: Optimize tool paths of flank milling with generic cutters based on approximation using the tool envelope surface, Computer-Aided Design, 41(12), 2009, 981–989. http://dx.doi.org/10.1016/j.cad.2009.06.013

[14] Maeng, S. R.; Baek, N.; Shin, S. Y. et al: A Z-map update method for linearly moving tools, Computer Aided Design, 35(11), 2003, 995–1009. http://dx.doi.org/10.1016/S0010-4485(02)00161-6

[15] Park, J. W.; Shin, Y. H.; Chung, Y. C.: Hybrid cutting simulation via discrete vector model, Computer Aided Design, 37(4), 2005, 419–430. http://dx.doi.org/10.1016/j.cad.2004.07.003

[16] Wang, D.; Chen, W. Y.; Li, T. et al: Five-Axis Flank Milling of Sculptured Surface with Barrel Cutters, Key Engineering Materials, 407, 2009, 292–297. http://dx.doi.org/10.4028/www.scientific.net/KEM.407-409.292

[17] Wang, W. P.; Wang, K. K.: Geometric modeling for swept volume of moving solids, IEEE Computer Graphics and Applications, 6(12), 1986, 8–17. http://dx.doi.org/10.1109/MCG.1986.276586

[18] Weinert, K.; Du, S. J.; Damm, P. et al: Swept volume generation for the simulation of machining processes, International Journal of Machine Tools & Manufacture, 44(6), 2004, 617–628. http://dx.doi.org/10.1016/j.ijmachtools.2003.12.003

[19] Yang, J. Z.; Abdel-Malek, K.: Approximate swept volumes of NURBS surfaces or solids, Computer Aided Geometric Design, 22(1), 2005, 1–26. http://dx.doi.org/10.1016/j.cagd.2004.08.002